minerals

MDPI

Article

Flotation Behaviors of Perovskite, Titanaugite, and Magnesium Aluminate Spinel Using Octyl Hydroxamic Acid as the Collector

Weiqing Wang [1,2,3,*], Yangge Zhu [3,*], Shiqiu Zhang [1], Jie Deng [4], Yang Huang [2] and Wu Yan [4]

1 School of Environment and Resource, Southwest University of Science and Technology, Mianyang 621010, Sichuan, China; swustzsq@sina.com
2 Key Laboratory of Solid Waste Treatment and Resource Recycle, Ministry of Education, Southwest University of Science and Technology, Mianyang 621010, Sichuan, China; swusthy@163.com
3 State Key Laboratory of Mineral Processing, Beijing General Research Institute of Mining and Metallurgy, Beijing 100260, China
4 Key Laboratory of Vanadium-Titanium Magnetite Comprehensive Utilization, Ministry of Land and Resources, Chengdu 610000, China; dengjie23@126.com (J.D.); yan507@126.com (W.Y.)
* Correspondence: swustwwq@sohu.com (W.W.); zhuyangge@bgrimm.com (Y.Z.); Tel.: +86-816-241-9569 (W.W.)

Received: 18 June 2017; Accepted: 28 July 2017; Published: 2 August 2017

Abstract: The flotation behaviors of perovskite, titanaugite, and magnesium aluminate spinel (MA-spinel), using octyl hydroxamic acid (OHA) as the collector, were investigated using microflotation experiments, zeta-potential measurements, Fourier transform infrared (FT-IR) analyses, X-ray photoelectron spectroscopy (XPS) analyses, and flotation experiments on artificially mixed minerals. The microflotation experiments show that the floatability of perovskite is clearly better than titanaugite and MA-spinel at around pH 5.5, while titanaugite possesses certain floatability at pH 6.0–6.5, and MA-spinel displays good floatability at pH > 8.0. The results of the FT-IR and XPS analyses show that OHA mainly interacts with Ti, resulting in perovskite flotation, and that the Al on titanaugite, as well as the Mg and Al on the MA-spinel surface, chemically react with OHA under acidic conditions. However, OHA mainly reacts with the Ti and Ca on the perovskite surface, Ca and Mg on the titanaugite surface, and Mg and Al on the MA-spinel surface under alkaline conditions. The results of the artificially mixed mineral flotation experiment show that the concentrate of TiO_2 grade increased from 19.73% to 30.18% at pH 5.4, which indicates that a weakly acidic solution is the appropriate condition for the flotation separation of perovskite from titanaugite and MA-spinel. The results of the modified slag flotation experiments show that the TiO_2 grade of concentrate increased from 18.13% to 23.88% at pH 5.4, through the open circuit test of "one roughing and one cleaning". OHA displays selectivity toward perovskite in the modified slag flotation, but the consumption of H_2SO_4 is very high. The $CaSO_4$ precipitate covered on the mineral surfaces results in poor TiO_2 grade and recovery.

Keywords: perovskite; titanaugite; magnesium aluminate spinel; octyl hydroxamic acid; flotation

1. Introduction

Titanium and titanium alloys are important strategic resources and can be widely used in various fields such as national defense, military, aerospace, aviation, navigation, and national economic production, owing to their excellent properties of low density, high strength, high temperature resistance, good low temperature resistance, and corrosion resistance [1,2].

The distribution of titanium resources in China is relatively concentrated, with more than 95% of titanium resource deposits around the PanXi region (Panzhihua and Xichang, Sichuan province) [3], which occurs in the form of vanadium-titanium magnetite with 8.7×10^8 t of TiO_2 [1,2,4].

Titanium resources exist in two types. In one type, the titanium in vanadium–titanium magnetite is partially substituted by iron, thus making it difficult to recover by magnetic separation. In the other type, the titanium occurs as granular ilmenite in the iron tailings during magnetic separation. The ilmenite can be effectively separated by floatation, and then the ilmenite concentrate is used for titanium dioxide preparation. When the vanadium–titanium magnetite concentrate was refined in a blast furnace, most of the titanium was concentrated into the blast furnace slag through a smelting process. The content of TiO_2 in the blast furnace slag can reach approximately 20%–25%, and the slag is referred to as Ti-bearing blast furnace slag, an important synthetic titanium resource [5,6]. At present, more than 3.0×10^6 t of titanium-bearing blast furnace slag is produced per year, which has already accumulated to 7.0×10^7 t [7]; the large quantities of slag results in the wastage of titanium resources and causes serious environmental pollution.

The main mineral components in the titanium-bearing blast furnace slag are perovskite, titanaugite (the peculiar pyroxene containing titanium in Panzhihua, a variant of diopside), Ti-rich diopside (another variant of diopside, the grade of TiO_2 was more than 17%), magnesium aluminate spinel (MA-spinel), and a small quantity of metallic Fe and Ti(C, N) [8]. Since the 1960s, several mineral processing and metallurgical methods had been applied to titanium-bearing blast furnace slag recycling, such as gravity separation, flotation combined with magnetic separation, smelting reduction, and hydrometallurgy [6,9,10]. However, because the dispersed distribution of the titanium component was in various fine-grained (<10 μm) mineral phases with complex interfacial combinations, the results of these above-mentioned methods to separate and enrich the titanium component may be poor. Facing these difficult problems, it was suggested [6,8,9,11] that we could concentrate the titanium component into one mineral, increase its crystalline size, and then separate the Ti-rich mineral from the modified titanium-bearing blast furnace slag. While perovskite was the higher TiO_2 grade mineral phase in titanium-bearing blast furnace slag, and it was suitable as the target mineral, some research indicated that selective precipitation of perovskite was one promising method to solve this problem.

According to the previous research, the perovskite selective precipitation process is as follows: the original slag was first pre-oxidized at 1050 °C for 45 min, and then the pre-oxidation samples were smelted at 1470 °C for 40 min, slowly cooled to 1350 °C at a cooling rate of 0.5 °C/min, and subjected to heat preservation for 120 min [12]. Figure 1 shows optical slice micrographs of the original and modified slag. After the selective precipitation processing, the main minerals in the modified slag were perovskite, titanaugite, and MA-spinel. The perovskite was transformed from a fine dispersive distribution to coarsening grains. The coarsening grain distribution of perovskite made it possible for flotation separation from the modified slag, and the key issue was the effective separation of perovskite from titanaugite and MA-spinel.

Alkyl hydroxamic acid is an effective collector for many oxide minerals flotation, including copper, iron, tin, niobite, and rare earth metal minerals [13–17]. The hydroxamate group could form chelates with many transition metal cations in bulk solutions. More specifically, the hydroxyl groups and the carbonyl groups in the hydroxamate formed a stable five-membered ring chelate with metal cations. The carbonyl group participated in the chelation by donating its lone pair electrons. Research has shown that they could also form chelates with metal atoms on mineral surfaces. Thus, Alkyl hydroxamic acid was capable of bonding with a mineral surface by "inner sphere adsorption" like carboxylic acids; however, the formed chelates are stronger than the coordination-bonded complex of the corresponding carboxylic acids. Moreover, results on separating perovskite from the modified slag using octyl hydroxamic acid (OHA) as the collector have not been frequently reported; it was only reported that perovskite can be separated by a flotation using hydroxamate as the collector and sodium silicate as the inhibitor, but the flotation mechanism has not been researched in detail [6].

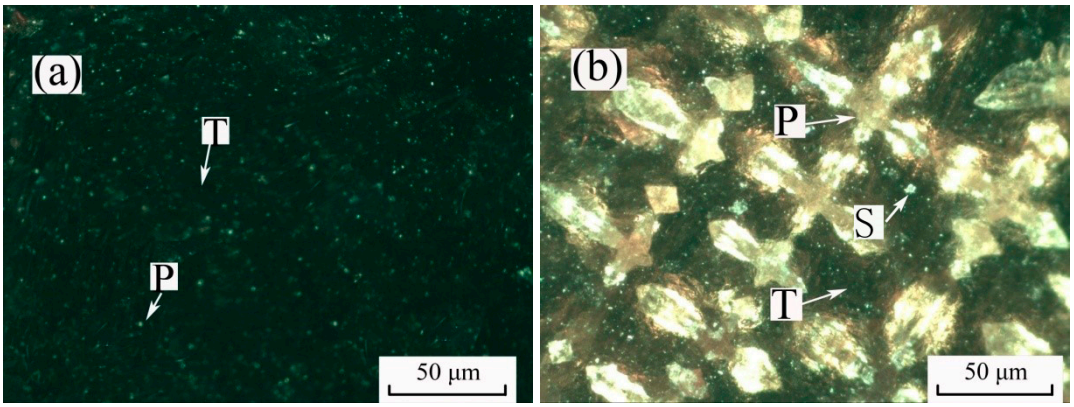

Figure 1. Optical micrographs of the original (**a**) and modified (**b**) slag (P: perovskite, T: titanaugite, S: magnesium aluminate spinel (MA-spinel)).

The objective of this work is to explore the flotation behaviors of perovskite, titanaugite, and MA-spinel in the modified titanium-bearing blast furnace slag, which are difficult to separate and purify by gravity separation or magnetic separation. Therefore, the pure minerals were synthesized based on our previous research [12]. To simulate the real mineral properties, the synthetic process of pure minerals was performed according to the heat treatment conditions of perovskite selective precipitation. The flotation behaviors of perovskite, titanaugite, and magnesium aluminate spinel use OHA as the collector through microflotation experiments, zeta-potential measurements, and Fourier transform infrared (FT-IR) and X-ray photoelectron spectroscopy (XPS) analyses.

2. Materials and Methods

2.1. Pure Minerals Synthesis

The pure minerals used in the experiments, including perovskite, titanaugite, and MA-spinel, are difficult to separate by physical methods from the modified titanium-blast furnace slag, because of their fine distribution granularity and complex association. Therefore, the chemical compositions of each mineral in the modified titanium-blast furnace slag were first analyzed by scanning electronic microscopy (SEM) equipped with energy dispersive X-ray (EDX) spectroscopy, the results of which are listed in Table 1.

Table 1. Chemical compositions of perovskite, titanaugite, and MA-spinel analyzed by EDX (mass fraction, %).

Sample	Tfe	TiO_2	SiO_2	Al_2O_3	CaO	MgO	Others	Total
Perovskite	0.72	54.85	0.61	0.25	42.63	0.13	0.81	100.00
Titanaugite	9.66	7.01	32.75	7.18	28.14	9.50	5.76	100.00
MA-spinel	0.31	0.01	0.56	73.69	0.60	24.20	0.63	100.00

Based on the chemical compositions of the above-mentioned three minerals, the pure minerals were artificially synthesized by high temperature solid-state methods using certain chemical oxides as the base materials under an air atmosphere. According to the authors' existing research results, the synthetic conditions are the same as the heat treatment process conditions of perovskite selective precipitation from titanium-blast furnace slag: the base materials were mixed thoroughly and smelted at 1470 °C for 40 min, slowly cooled to 1350 °C at a cooling rate of 0.5 °C/min, and subjected to heat preservation for 120 min [12]. The synthetic perovskite, titanaugite, and MA-spinel samples were then dry-ground in a ball mill and washed three times using deionized water. Consequently, high-purity minerals were obtained, and the particle size distribution results of the pure perovskite,

titanaugite, and MA-spinel samples (detected by a laser diffraction particle size analyzer, Beckman Coulter, LS13320, Brea, CA, USA) are shown in Figure 2.

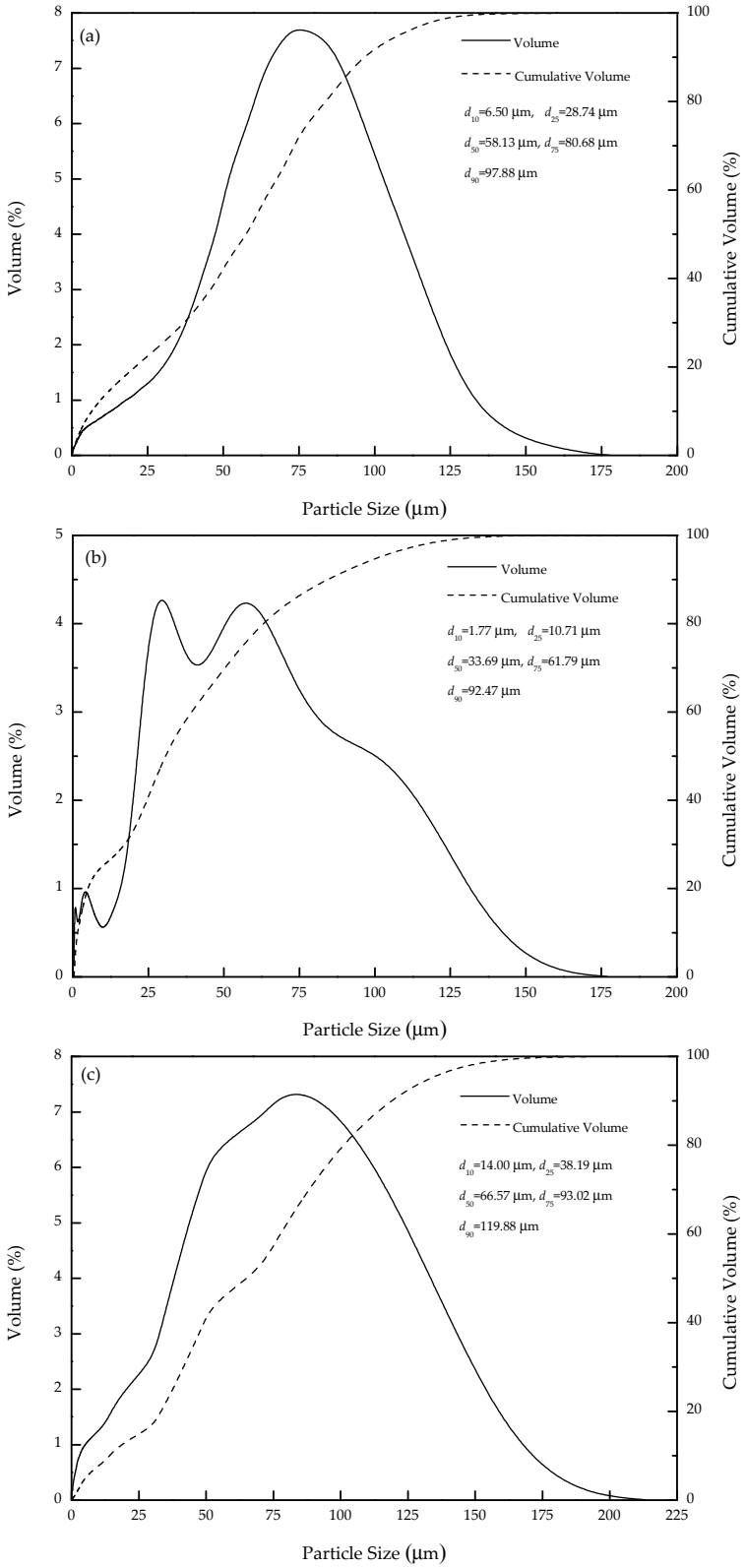

Figure 2. Particle size distribution of the synthetic perovskite (**a**), titanaugite (**b**), and MA-spinel (**c**).

Figure 3 shows the X-ray diffraction (XRD) spectra of the synthetic perovskite, titanaugite, MA-spinel, and modified slag samples.

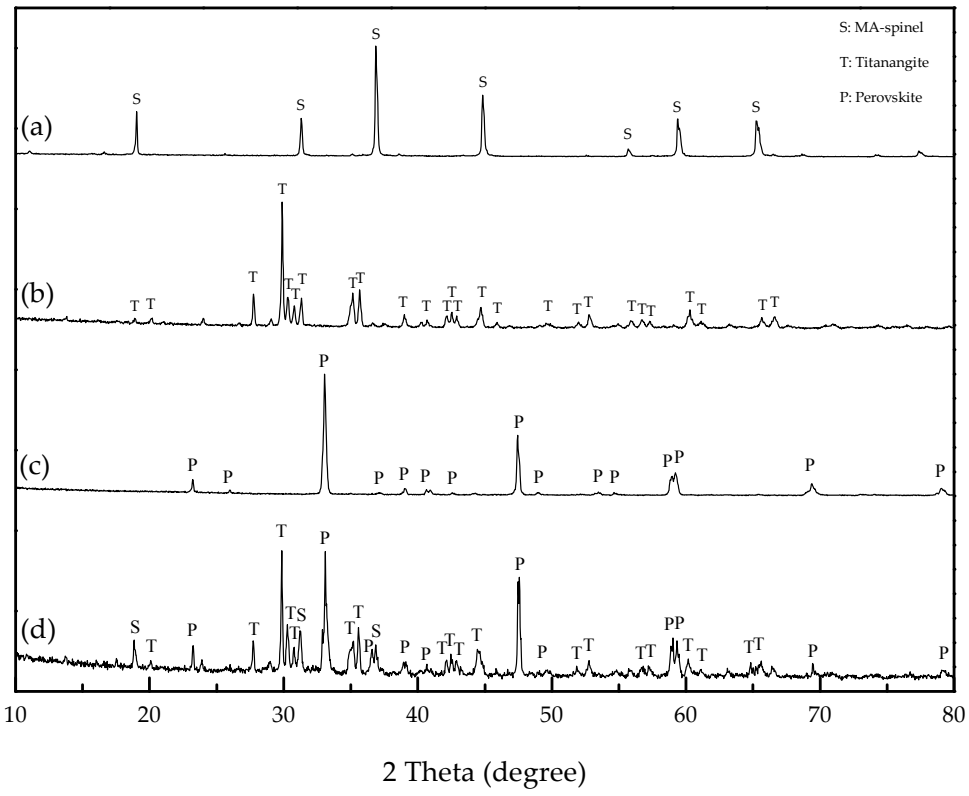

Figure 3. XRD spectra of the synthetic MA-spinel (**a**), titanaugite (**b**), perovskite (**c**), and modified slag (**d**).

The XRD spectrum of modified titanium-blast furnace slag shows that the main mineral components include perovskite, titanaugite, and MA-spinel (Figure 3d). The XRD spectra of the three synthetic pure minerals indicate that the diffraction peaks of perovskite, titanaugite, and MA-spinel are well matched with the pattern of standard diffraction peaks: perovskite (No. 22-153), titanaugite (No. 24-203), and MA-spinel (No. 21-1152). According to the results of the XRD analysis, the purities of synthetic perovskite, titanaugite, and MA-spinel were very high, indicating that the synthetic pure minerals could simulate the relevant minerals in the modified slag with similar compositions and crystal structures.

2.2. Reagents

Octyl hydroxamic acid (OHA, 99%, $CH_3(CH_2)_6CONHOH$) was used as the collector for the microflotation tests and the modified slag flotation experiments. Sulfuric acid (H_2SO_4) or sodium hydroxide (NaOH) was used for the pH adjustment of aqueous suspensions in the experiments. All the chemicals were of analytical grade, and the water used for all the experiments was deionized water with a resistivity of 18.25 MΩ·cm.

2.3. Microflotation Experiments

Microflotation experiments were performed in a 40-mL hitch groove flotation cell. The Plexiglas cell was filled with 2.0 g pure mineral particles, and then 35 mL deionized water was added. The pH of the suspension was adjusted by H_2SO_4 or NaOH for 3 min. Then, the collector was added and agitated for an additional 3 min, and the pH of the suspension was recorded before the flotation. The

flotation was conducted for 4 min. The recoveries were calculated by the weight of the concentrates after filtering and drying. Three measurements in the microflotation experiment were made, and their averages were taken as the results.

2.4. Zeta-Potential Measurements

The Zeta-potentials of the pure mineral particles were measured using a Zetasizer Nano Zs90 (Malvern Instruments, Worcestershire, UK) at room temperature (25 °C). They were monitored continuously in terms of the conductivity and pH of the suspension during the measurement. The purified mineral particles were ground to a size of 2 μm using an agate mill. The suspension was prepared by adding 30 mg of the purified mineral particles to 50 mL of deionized water. The prepared suspension was conditioned by magnetical stirring for 5 min, during which the pH of the suspension was measured. After settling for 10 min, the supernatant of the dilute fine particle suspension was obtained for zeta-potential measurements. Three measurements of zeta potentials were obtained, and their averages were taken as the results.

2.5. FT-IR Spectroscopy Analyses

The FT-IR spectra were obtained using a Spectrum One (Version BM) FT-IR (PerkinElmer, Waltham, MA, USA) spectrometer to characterize the nature of the interaction between the collector and minerals. Approximately 10% (mass fraction) of the solid sample was mixed with spectroscopic grade KBr. The wavenumber range of the spectra was 400–4000 cm^{-1}. The spectra were recorded with 32 scans measured at 2 cm^{-1} resolution. The purified mineral particles (2.0 g) were placed in a Plexiglas cell with H_2SO_4 or NaOH as the pH-regulating reagent. Next, the purified samples were conditioned for another 3 min with OHA (1.5×10^{-4} M). Subsequently, the solid samples were washed three times using deionized water with the same pH. The washed samples for FT-IR analysis were vacuum-dried at 50 °C.

2.6. XPS Analyses

The XPS analyses were performed using a Kratos AXIS Ultra XPS system equipped with a monochromatic Al X-ray source operated at 150 W (the energy resolution is 0.48 eV (Ag 3d5/2) and the error value is 0.05 eV). Each analysis started with a survey scan from 0 to 1350 eV with a dwell time of 8 s and bandpass energy of 150 eV in steps of 1 eV, with one sweep performed. For the high-resolution analysis, the number of sweeps was increased, the bandpass energy was lowered to 30 eV in steps of 50 meV, and the dwell time was reduced to 0.5 s.

The purified mineral particles (2.0 g) were placed in a Plexiglas cell with H_2SO_4 or NaOH as the pH-regulating reagent. Subsequently, the purified samples were conditioned for another 3 min with OHA (1.5×10^{-4} M). Next, the solid samples were washed three times using the deionized water with the same pH. The washed samples for XPS analysis were vacuum-dried at 50 °C.

2.7. Artificially Mixed Mineral Flotation Experiments

The artificially mixed minerals were mixed to include 0.67 g pure perovskite, 0.67 g pure titanaugite, and 0.67 g pure MA-spinel. The artificially mixed mineral flotation experiments were performed in a 40-mL hitch groove flotation cell. The artificially mixed mineral (2.01 g) was placed in a Plexiglas cell, which was then filled with 35 mL of deionized water. The pH of the suspension was adjusted by H_2SO_4 or NaOH for 3 min, the collector (1.5×10^{-4} M) was added and agitated for 3 min, and then the pH of the suspension was measured before the flotation. The flotation was conducted for 4 min. The concentrates and the tailings were weighed after filtering and drying, and then separately sampled to analyze the grade of TiO_2 by the chemical analysis method. The flotation recoveries of the concentrates and the tailings were calculated based on the yield and the grade of TiO_2. The average value from three flotation experiments under the same conditions was used as the result of the artificially mixed mineral flotation.

2.8. Modified Slag Flotation Experiments

The modified slag flotation experiments were performed in a 0.5-L flotation cell. Modified slag amounting to 100.0 g (the particle size distribution d_{90} = 32.76 μm) was placed in a Plexiglas cell filled with deionized water. The pH of the suspension was adjusted by H_2SO_4 or NaOH for 3 min. Then, the collector (500 g/t) was added and agitated for 3 min, and the pH of the suspension was measured before the flotation. The flotation was conducted for 4 min, and then the open circuit test of "one roughing and one cleaning" was carried out. The concentrates and the tailings were weighed after filtering and drying, and the grade of TiO_2 was analyzed by the chemical analysis method. The flotation recoveries of the concentrates and the tailings were calculated based on the yields and the grades of TiO_2.

3. Results and Discussion

3.1. Microflotation

Figure 4 shows the flotation recoveries of perovskite, titanaugite, and MA-spinel as functions of pH using OHA as the collector (c_{OHA} = 0.5 × 10^{-4} M). The results indicate that the recovery of perovskite first increased and then decreased with increasing pH, and the maximum recovery occurred at approximately pH 5.5. The floatability of perovskite is clearly better than that of titanaugite and MA-spinel at pH < 6.5. Titanaugite possesses certain floatability at pH 6.0–6.5, and MA-spinel displays good floatability at pH > 8.0, particularly at pH ≥ 10.

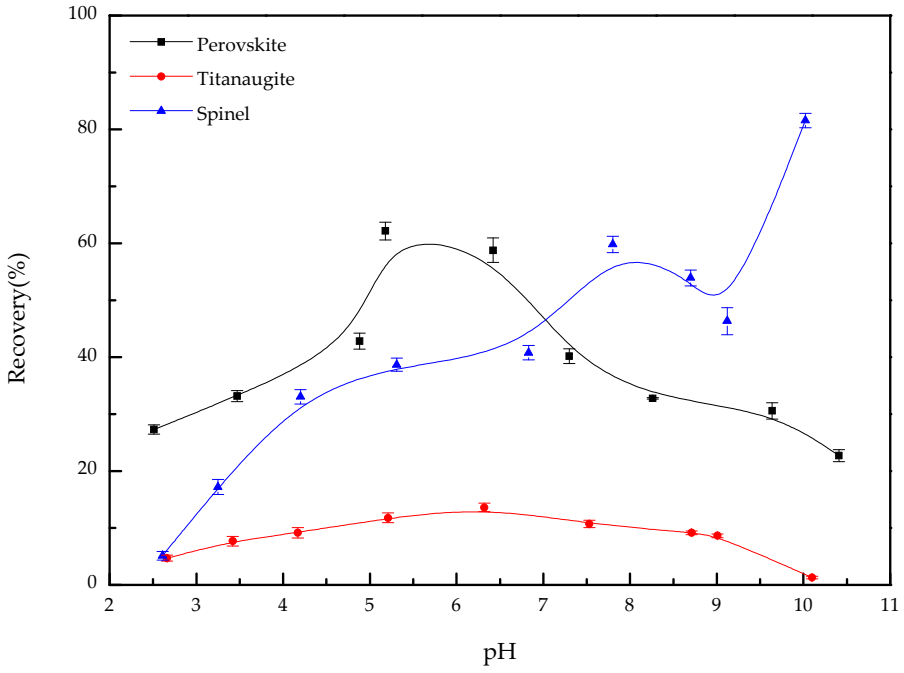

Figure 4. Flotation recovery of minerals as functions of pH (c_{OHA} = 0.5 × 10^{-4} M).

Figure 5 shows that the increase of OHA concentration clearly increased the flotation recoveries of perovskite, titanaugite, and MA-spinel. However, the flotation recoveries of the three minerals increased slowly with excess of 1.5 × 10^{-4} M OHA, and the floatability of perovskite can reach 75.93%, which is better than that of titanaugite and MA-spinel. Therefore, this OHA concentration (1.5 × 10^{-4} M) was used in all the microflotation experiments.

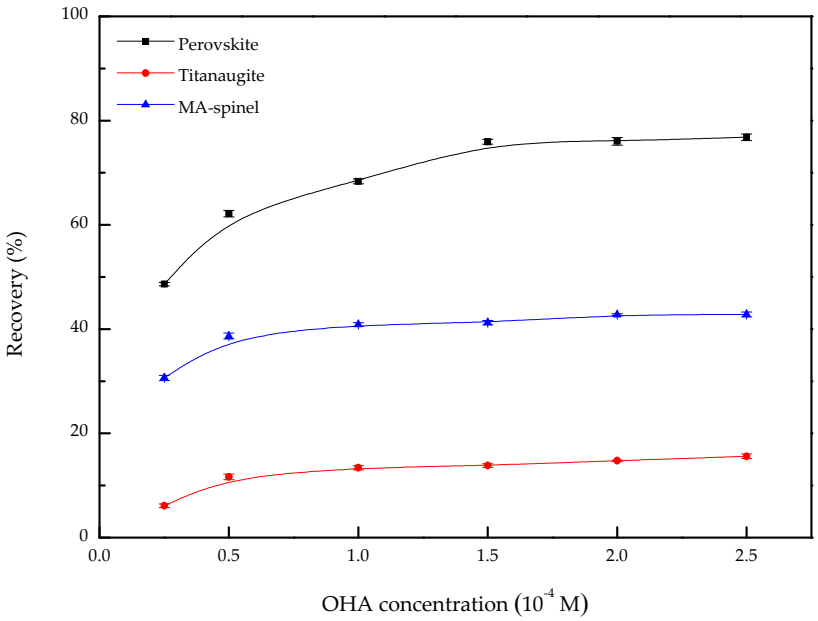

Figure 5. Flotation recovery of pure minerals as functions of octyl hydroxamic acid (OHA) concentration (pH = 5.0−5.5).

3.2. Zeta-Potential

Figure 6 presents the zeta-potentials of perovskite, titanaugite, and MA-spinel in the absence and presence of OHA as a function of pulp pH value. In the absence of OHA, the results indicate that the point of zero charges (PZCs) of perovskite, titanaugite, and MA-spinel are located at around pH 4.1, 3.5, and 8.6, respectively. In the presence of OHA, the zeta-potentials of perovskite, titanaugite, and MA-spinel are negative in the pH range, except that perovskite is positive at pH = 2.4 (12.6 mV). The decrease in the zeta-potentials of perovskite, titanaugite, and MA-spinel can be attributed to the specific adsorption of OHA onto mineral surfaces (Helmholtz layer); it is probable that coordination reactions are involved [18].

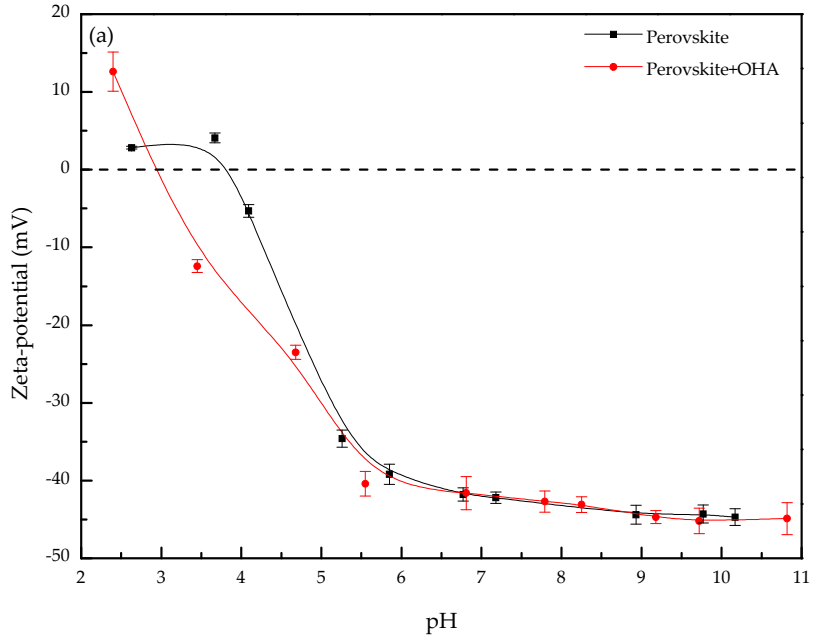

Figure 6. *Cont.*

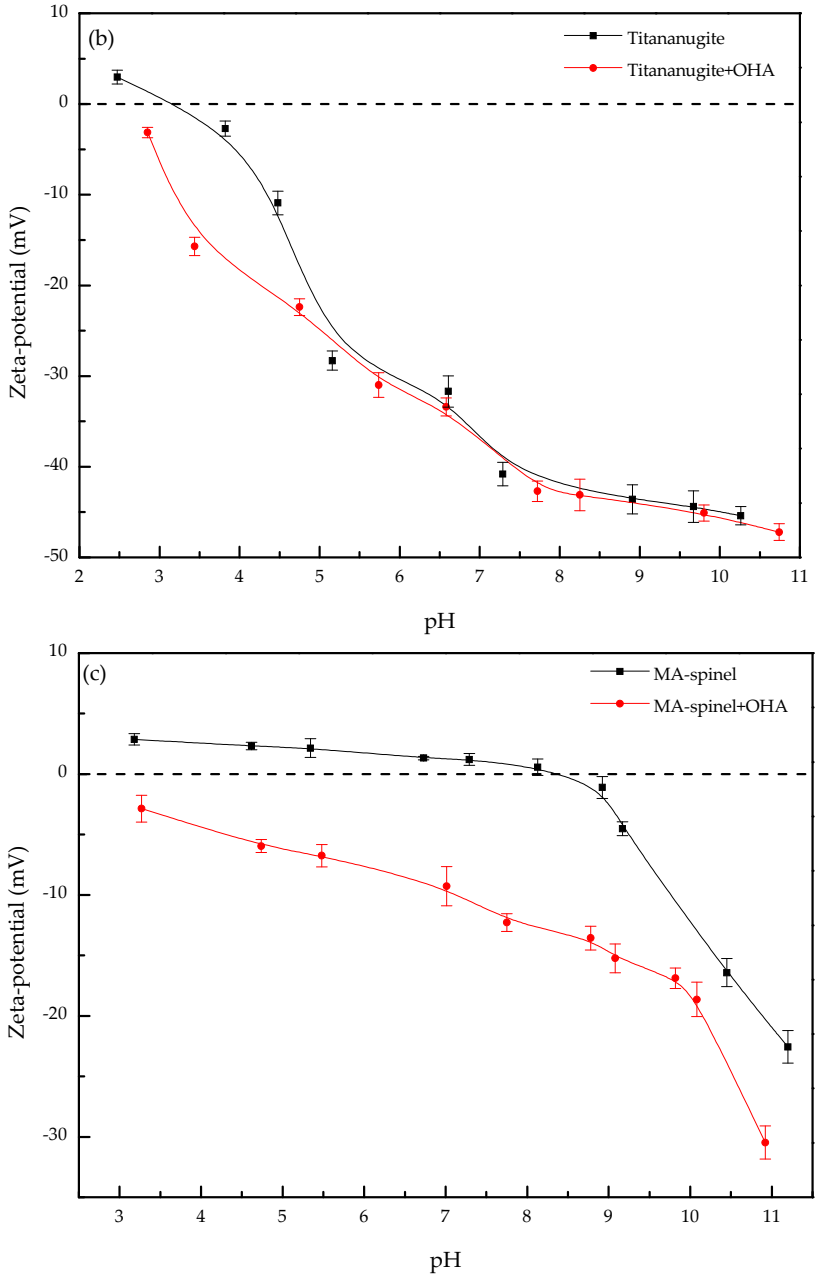

Figure 6. Zeta-potentials of perovskite (**a**), titanaugite (**b**), and MA-spinel (**c**) functions of pH in the absence and presence of OHA (c_{OHA} = 1.5 × 10^{-4} M).

3.3. FT-IR Analysis

Figure 7 shows the FT-IR spectra of perovskite and perovskite with OHA at different pH levels. To understand the interaction between OHA and minerals, the FT-IR spectrum of OHA was also measured. In the FT-IR spectrum of OHA, the band at 3257.9 and 1624.2 cm^{-1} can be attributed to the –OH stretching vibration and the out-of-plane bending vibration of the –N–OH group, respectively. The bands at 2915.9 and 2847.1 cm^{-1} can be attributed to the C–H stretching vibration of the $–CH_2–$ and $–CH_3$ groups, respectively. The band at 1468.3 cm^{-1} can be attributed to the C–H scissor bending vibration of the $–CH_2–$ group, and the band at 1424.0 cm^{-1} can attributed to the C–H antisymmetric deformation vibration of the $–CH_3$ group. The band at 722.7 cm^{-1} can be attributed to the $–(CH_2)_n–$ deformation vibration. Among these bands, that at 1663.6 cm^{-1} can be attributed to the C=O stretching

vibration. However, that at 1566.8 cm^{-1} can be attributed to the –N–H stretching vibration, and the bands at 1078.8, 1031.3, and 970.3 cm^{-1} can be attributed to the N–O stretching vibration [19–21].

In the FT-IR spectrum of perovskite, the band at 574.1 and 446.4 cm^{-1} can be attributed to the Ti−O stretching and Ti−O−Ti bridge stretching modes [22,23], and that at 3433.3 cm^{-1} belongs to the bending vibration of the O–H band in hydroxyls and water adsorbed on perovskite surfaces [22,23]. The FT-IR spectra of perovskite with OHA at different pH levels show additional C–H, C=O, and N–O stretching intensities for OHA compared with the pure perovskite. At pH 5.4, the new bands at 2919.4 and 2851.2 cm^{-1} can be attributed to the C–H stretching vibrations, and the band at 1448.9 cm^{-1} is C–H antisymmetric deformation vibration of $–CH_3$ group. These frequency bands do not change clearly, but it indicates that OHA was adsorbed onto the perovskite surface. The band at 1630.6 cm^{-1} is the C=O stretching vibration, and the band at 873.9 cm^{-1} can be attributed to the N–O stretching vibration, which shifted to lower wavenumbers by and 96.4 cm^{-1}, respectively. These results imply chemisorption of OHA on perovskite surfaces. A similar situation was observed at pH 9.3.

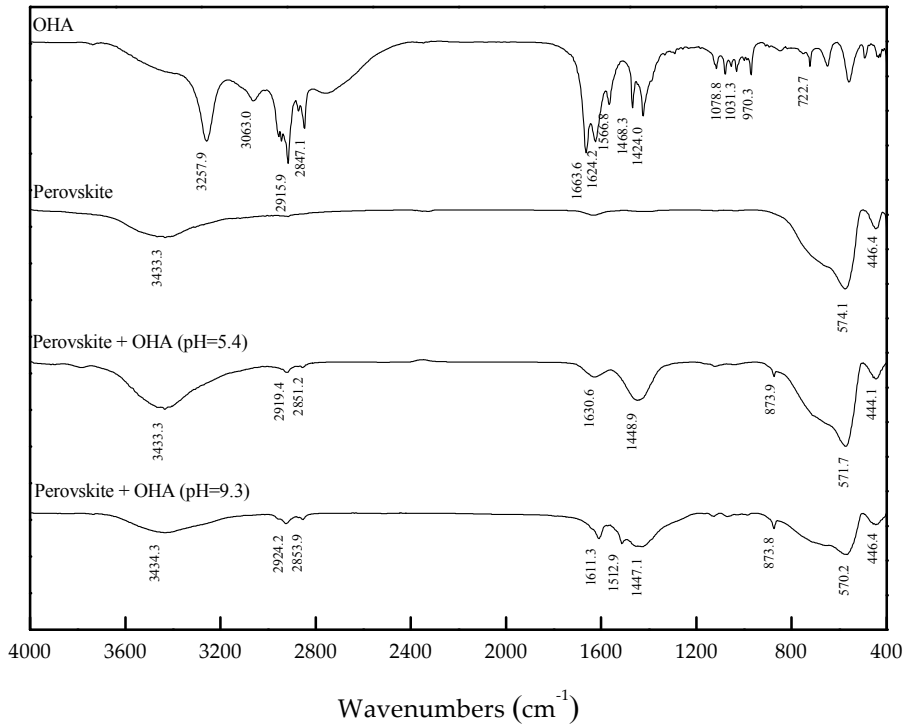

Figure 7. FT-IR spectra of the OHA and perovskite with OHA at different pH levels.

Figure 8 shows the FT-IR spectra of titanaugite and titanaugite with OHA at different pH levels. At pH 5.4, the new bands at 2927.2 and 2853.1 cm^{-1} were previously attributed to the C–H stretching vibration of OHA. The band at 1636.2 cm^{-1} was C=O stretching vibration, and the band at 898.6 cm^{-1} was N–O stretching vibration, which shifted to lower wavenumbers by 27.4 and 71.7 cm^{-1}, respectively, compared to that in the FT-IR spectrum of OHA. These results indicate that OHA reacted on titanaugite surface surfaces. A similar situation was observed at pH 9.3.

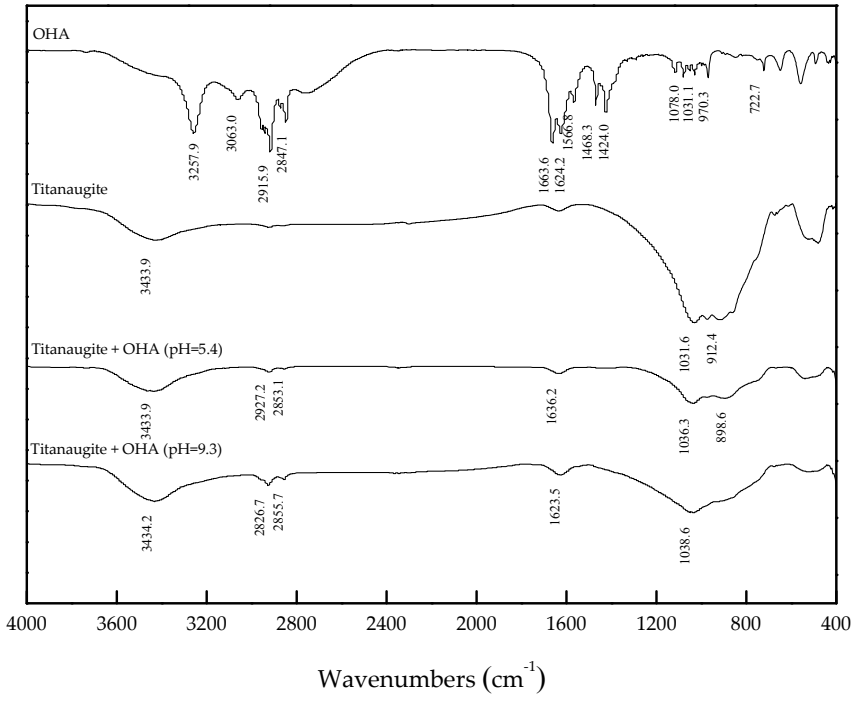

Figure 8. FT-IR spectra of the OHA and titanaugite with OHA at different pH levels.

Figure 9 shows the FT-IR spectra of MA-spinel and MA-spinel with OHA at different pH levels. Similar to perovskite and titanaugite, the new bands attributed to the C–H stretching vibration indicate that OHA was adsorbed onto MA-spinel surface. The band at 1629.9 cm^{-1} was C=O stretching vibration, and the band at 1121.6 cm^{-1} was N–O stretching vibration, which shifted to lower wavenumbers by 33.7 cm^{-1} and a higher by 42.8 cm^{-1}, respectively. A similar situation was observed at pH 9.3 and the results indicate that OHA reacted on MA-spinel surfaces.

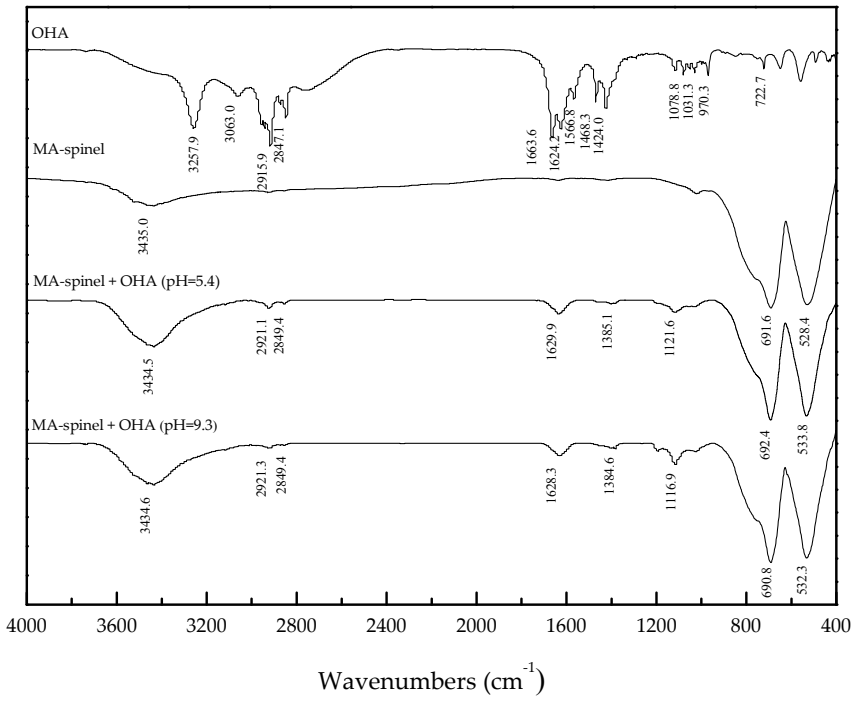

Figure 9. FT-IR spectra of the OHA and MA-spinel with OHA at different pH levels.

3.4. XPS Analysis

The XPS analyses were performed to further confirm that OHA mainly interacts with perovskite, titanaugite, and MA-spinel in different pH level solutions. Table 2 presents the binding energies of elements on perovskite surfaces before and after the interactions with OHA.

Table 2. Binding energies of elements on perovskite surface.

Sample	Binding Energy (eV)			Chemical Shift (eV)		
	C1s	Ti2p	Ca2p	C1s	Ti2p	Ca2p
H_2SO_4 (pH = 5.4)	284.79	458.15	346.15	-	-	-
H_2SO_4 + OHA (pH = 5.4)	284.84	458.52	346.18	+0.05	+0.37	+0.03
NaOH (pH = 9.3)	284.79	458.12	346.10	-	-	-
NaOH + OHA (pH = 9.3)	284.80	458.00	346.21	+0.01	−0.12	+0.11

After perovskite was treated by OHA, the chemical shifts of Ca were not clear, while that of Ti reached +0.37 eV under acidic conditions (pH = 5.4). The binding energies of Ca and Ti reached −0.12 and +0.11 eV, respectively, under alkaline conditions (pH = 9.3). The relative contents of the elements on perovskite surfaces in the absence and presence of OHA, as measured by XPS, are listed in Table 3. After perovskite was treated by OHA under acidic conditions, the relative contents of Ti and Ca decreased to 1.85% and 0.69%, respectively. The relative content of Ti and Ca decreased to 2.12% and 1.25%, respectively, under alkaline conditions. According to the binding energy shifts and the relative contents of Ti and Ca, these results indicate that OHA mainly interacted with Ti under acidic conditions, but interacted with both Ti and Ca under alkaline conditions.

Table 3. Relative contents of elements on perovskite surface.

Sample	Surface Atomic Composition (%)		
	C1s	Ti2p	Ca2p
H_2SO_4 (pH = 5.4)	61.54	17.58	14.95
H_2SO_4 + OHA (pH = 5.4)	70.01	15.73	14.26
NaOH (pH = 9.3)	58.98	18.13	14.75
NaOH + OHA (pH = 9.3)	70.49	16.01	13.50

Table 4 gives the binding energies of elements on titanaugite surfaces before and after the interactions with OHA. After titanaugite was treated by OHA, the chemical shifts of the elements indicate that the OHA reacted on the surface of titanaugite. The relative contents of elements on the surface of titanaugite in the absence and presence of OHA, as measured by XPS, are listed in Table 5. After titanaugite was treated by OHA under acidic conditions, the main element on the titanaugite surface was Al, and the relative contents of Ca, Mg, Ti, and Al decreased to 0.13%, 0.53%, 0.94%, and 5.24%, respectively. This result indicates that OHA mainly interacted with Al under acidic conditions. A similar situation was observed under alkaline conditions. The relative contents of Ca, Mg, Ti, and Al decreased to 7.23%, 2.47%, 1.33%, and 1.63%, respectively. These results indicate that OHA mainly interacted with Ca and Mg under alkaline conditions.

Table 4. Binding energies of elements on titanaugite surface.

Samples	Binding Energy (eV)					Chemical Shift (eV)				
	C1s	Ca2p	Mg1s	Ti2p	Al2p	C1s	Ca2p	Mg1s	Ti2p	Al2p
H_2SO_4 (pH = 5.7)	284.76	347.51	1304.26	458.84	74.09	-	-	-	-	-
H_2SO_4 + OHA (pH = 5.7)	284.80	347.59	1304.57	458.96	74.36	+0.04	+0.08	+0.31	+0.12	+0.25
NaOH (pH = 10.7)	284.82	347.55	1304.40	459.04	74.20	-	-	-	-	-
NaOH + OHA (pH = 10.7)	284.83	347.96	1304.34	459.85	74.20	+0.01	+0.41	−0.16	−0.09	0.00

Table 5. Relative contents of elements on titanaugite surface.

Sample	Surface Atomic Composition (%)				
	C1s	Ca2p	Mg1s	Ti2p	Al2p
H_2SO_4 (pH = 5.7)	61.56	7.33	3.92	3.05	21.03
H_2SO_4 + OHA (pH = 5.7)	71.51	7.20	3.39	2.11	15.79
NaOH (pH = 10.7)	58.27	13.68	4.00	6.17	17.89
NaOH + OHA (pH = 10.7)	71.92	6.45	1.53	4.84	15.26

Table 6 presents the binding energies of elements on the MA-spinel surface before and after the interactions with OHA. After MA-spinel was treated by OHA, the chemical shifts of the elements indicate that the OHA reacted on the surface of MA-spinel. The relative contents of elements on the surface of MA-spinel in the absence and presence of OHA, as measured by XPS, are listed in Table 7. According to the binding energy and relative element content of Mg and Al, OHA mainly interacted with Mg and Al in the entire pH range.

Table 6. Binding energies of elements on MA-spinel surface.

Sample	Binding Energy (eV)			Chemical Shift (eV)		
	C1s	Mg1s	Al2p	C1s	Mg1s	Al2p
H_2SO_4 (pH = 5.3)	284.76	1303.93	74.06	-	-	-
H_2SO_4 + OHA (pH = 5.3)	284.80	1304.21	74.15	+0.04	+0.28	+0.11
NaOH (pH = 9.4)	284.81	1304.07	74.19	-	-	-
NaOH + OHA (pH = 9.4)	284.80	1303.97	74.13	−0.01	−0.10	−0.06

Table 7. Relative contents of elements on MA-spinel surface.

Sample	Surface Atomic Composition (%)		
	C1s	Mg1s	Al2p
H_2SO_4 (pH = 5.3)	45.68	9.4	44.91
H_2SO_4 + OHA (pH = 5.3)	47.05	8.54	44.41
NaOH (pH = 9.4)	43.61	10.83	45.56
NaOH + OHA (pH = 9.4)	44.54	9.91	45.55

3.5. Interaction Mechanism of OHA and Minerals

At different pH environments, the pulp collector exhibited different forms during the flotation process, and the existing forms of the collector further affected the flotation behaviors of the minerals. The following are the balanced equations and equilibrium constants of OHA.

$$\mathrm{RCONHOH} \rightarrow \mathrm{RCONHO^-} + \mathrm{H^+}, K_\alpha = [\mathrm{RCONHO^-}][\mathrm{H^+}]/[\mathrm{RCONHOH}]$$

According to the ionization constant pK_α of OHA ≅ 9 [24], the solution chemistry of OHA can be calculated to generate the concentration logarithmic diagram of each component in different pH solutions. Figure 10 shows the logC−pH of the OHA hydrolysis components as functions of pH when the OHA concentration was 1.5×10^{-4} M. It can be seen that the ionic OHA concentration gradually increased, but the molecule OHA concentration decreased with increasing pulp pH. When $pH < pK_\alpha = 9$, the OHA molecule (RCONHOH) was the predominant species in the flotation pulp, and the OHA anion ($RCONHO^-$) was prominent when pH > 9. In the OHA aqueous solution, the OHA ion and OHA molecule would adsorb on the mineral surface together, and the OHA ion would chelate with the metal cations on the mineral surface, as well as the nonpolar part of the OHA molecule adsorbing the former OHA ion by hydrogen bond. Hence, the ion-molecule coadsorption increased the OHA activity and promoted good collecting ability.

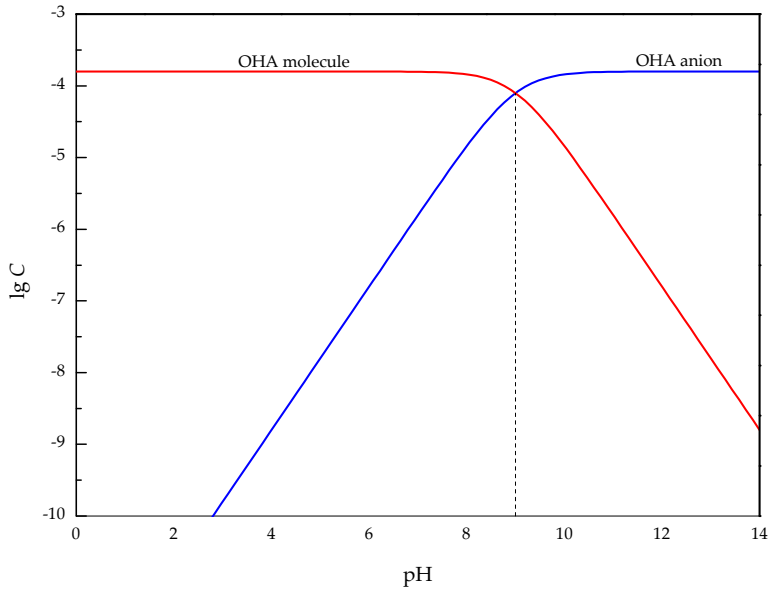

Figure 10. Logarithmic diagram of octyl hydroxamate acid hydrolysis components (c_{OHA} = 1.5 × 10^{-4} M).

As shown in Figure 4, perovskite has its maximum recovery at approximately pH 5.5, similar to the report of Ma [25], and its floatability is better than those of titanaugite and MA-spinel. Similar to ilmenite in the flotation pulp, the unsaturated Ca^{2+} ions and Ti^{4+} ions on the perovskite surface were combined with OH^- ions and formed a series of hydroxyl complex compounds. Under a weak acid condition, most of the Ca^{2+} ions were dissolved from the perovskite surface. Also, the remaining metallic ions were mainly Ti^{4+} ions in the forms of Ti(OH)+ 3 and Ti(OH)2+ 2 [26,27], which performed as the active sites on which OHA molecules were adsorbed (the chemical shift of Ti2p reached +0.37 eV, Table 2), and resulted in the maximum recovery of perovskite. The main chemical compositions of titanaugite were Ca^{2+} ions, Mg^{2+} ions, and Al^{3+} ions. Under the weak acid pulp condition, most of the Ca^{2+} ions and Mg^{2+} ions were dissolved from the titanaugite surface, and the remaining metallic ions were mainly Al^{3+} ions (Table 5), in the forms of $Al(OH)_3$ [28], as the active sites on which OHA molecules were adsorbed; this resulted in a remarkable chemical shift of Al2p (+0.25 eV, Table 4). The chemical compositions of MA-spinel were only Mg^{2+} ions and Al^{3+} ions; under the weak acid pulp, a portion of the Mg^{2+} ions were dissolved, and the remaining metallic ions were still Mg^{2+} ions and Al^{3+} ions (Table 7). The subsequent hydroxyl complex compounds could perform as the active sites on which OHA were adsorbed, and resulted in a remarkable chemical shift of Mg1s and Al2p (+0.28 eV, +0.11 eV, Table 6). Under alkaline condition, Mg^{2+} ions and Al^{3+} ions were difficult to dissolve from the minerals' surfaces, and the active sites on which OHA were adsorbed would still be Mg and Al. According to the results of the FT-IR and XPS analyses, the proposed adsorption model of OHA on the minerals' surfaces is presented in Figure 11.

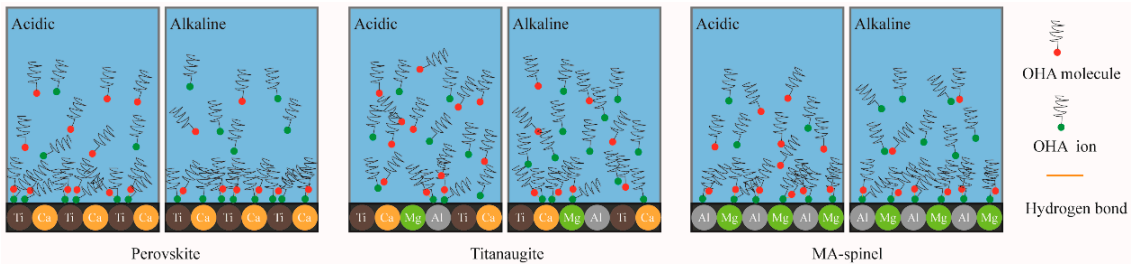

Figure 11. Proposed adsorption model of OHA reacted on perovskite, titanaugite, and MA-spinel surface in different pH solutions.

3.6. Artificially Mixed Mineral Flotation

The artificially mixed mineral flotation experiments were investigated at pH 5.4 and 9.3, with the results shown in Figure 12. The results indicate that the concentrate of TiO_2 grade increased from 19.73% to 30.18% at pH 5.4 but decreased to 19.09% at pH 9.3. The artificially mixed mineral flotation results indicate that OHA possessed good selectivity toward perovskite separated from titanaugite and MA-spinel at pH 5.4 (weak acidic condition), and these results are consistent with the results of the microflotation experiments.

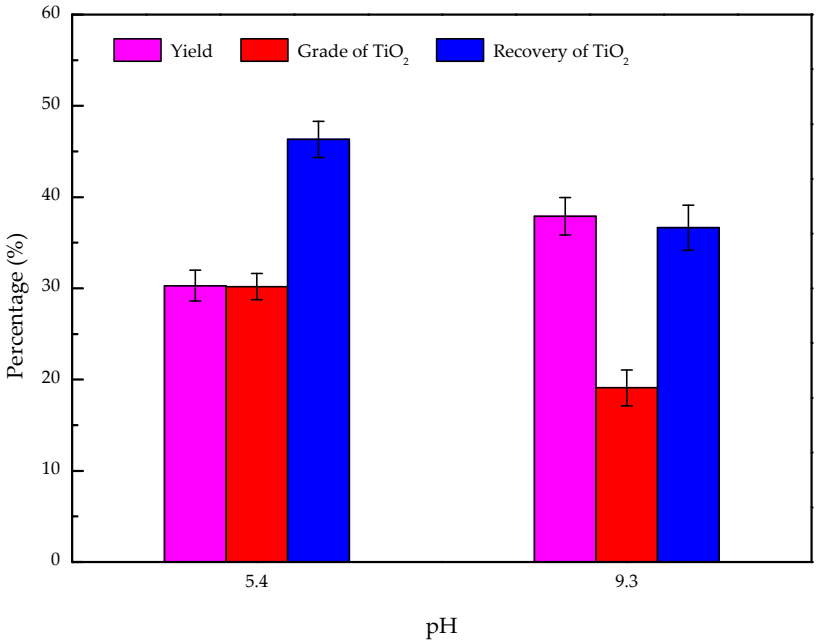

Figure 12. The yields, TiO_2 grades, and recoveries of the concentrates from artificially mixed mineral flotation at different pH levels.

3.7. Modified Slag Flotation

The flotation experiments on modified slag were investigated at pH levels of 5.4 and 9.3. The results of the modified slag flotation experiments are shown in Figure 13. The results indicate that the concentrate of TiO_2 grade increases from 18.13% to 23.88% at pH 5.4, and OHA certainly displays selectivity to perovskite in the modified slag flotation, but is worse than the artificially mixed mineral flotation at the same pH condition, and the consumption of H_2SO_4 is very large (up to 16.31 kg/t). At pH 9.3, the TiO_2 grade of concentrate is only 19.42%, close to the feed (modified slag). According to the artificially mixed mineral flotation experiments results, it is certain that the perovskite flotation from modified slag should be under a weak acid condition. In order to determine the reasons for the poor selectivity at pH 5.3, the Ca^{2+} ion concentration of the pulp after agitation for 3 min was measured by inductively coupled plasma atomic emission spectroscopy.

The results show that the Ca^{2+} ion concentration reaches to 634 mg/L, and it can also be inferred that a certain amount of free CaO exists in the modified slag. Further SEM analysis of the concentrate obtained at pH 5.4 was conducted, and a SEM micrograph and EDX spectrum are shown in Figure 14. It can be seen that the mineral grain surfaces, perovskite (Figure 14a), Titanaugite (Figure 14b), and MA-spinel (Figure 14c) were coated by many needle particles; the EDX spectrum indicated the needle particles constituted $CaSO_4$ (Figure 14d). The existing free CaO in the modified slag reacted with H_2SO_4 and the $CaSO_4$ precipitate covered the minerals' surfaces during the flotation process, similar to certain research reports [29,30]. These may be the main factors resulting in the large H_2SO_4 consumption and

poor TiO_2 grade and recovery. Therefore, methods to effectively separate perovskite from the gangue in the modified slag by flotation need to be further researched.

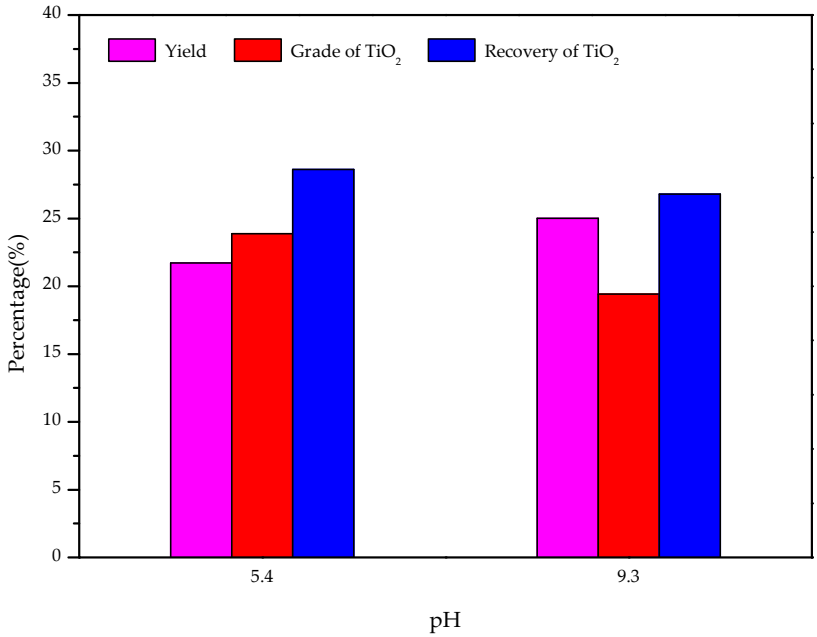

Figure 13. The yields, TiO_2 grades, and recoveries of the concentrates from modified slag flotation at different pH levels.

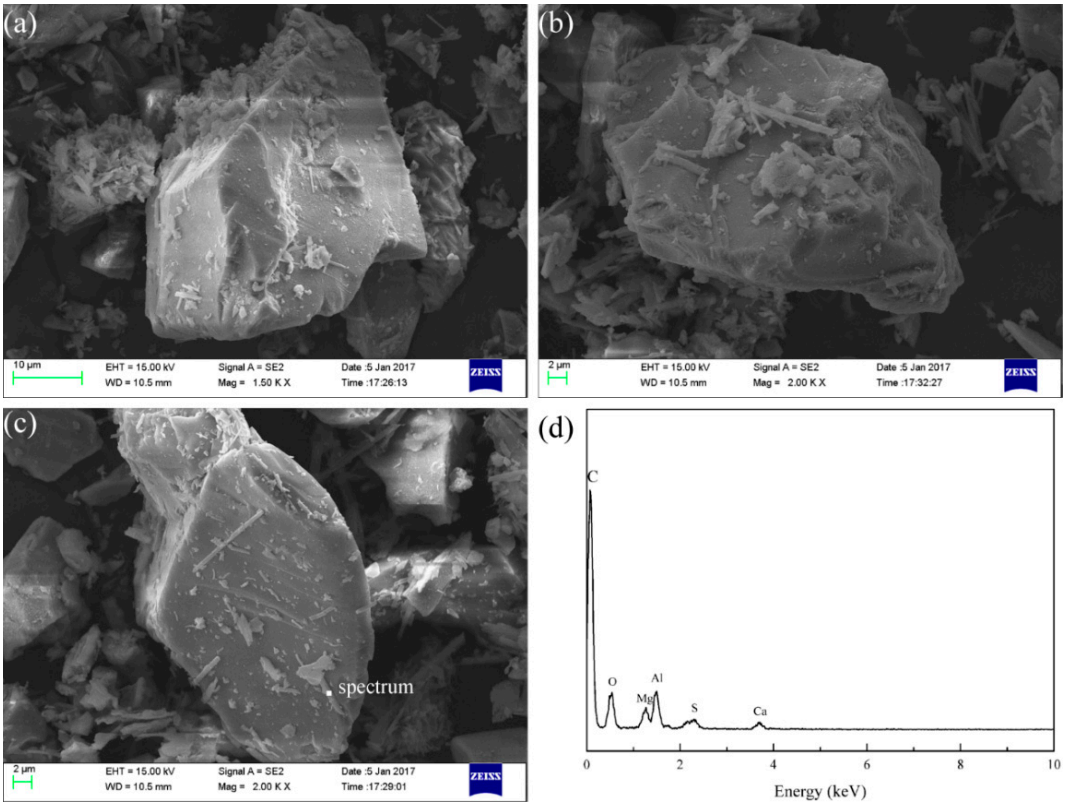

Figure 14. Scanning electronic microscopy (SEM) micrograph of perovskite (**a**), Titanaugite (**b**), MA-spinel (**c**), and EDX spectrum of needles coated on minerals' surfaces (**d**).

4. Conclusions

(1) When OHA was used as the collector, the floatability of perovskite is clearly better than that of titanaugite and MA-spinel at approximately pH 5.5. Titanaugite possesses certain floatability at pH 6.0–6.5, and MA-spinel displays good floatability at pH > 8.0.

(2) The large decrease in the zeta-potentials of perovskite, titanaugite, and MA-spinel can be attributed to the specific adsorption of OHA onto the Helmholtz layer of the mineral surfaces.

(3) Under acidic conditions, OHA mainly interacted with Ti, resulting in perovskite flotation; additionally, the Al on the titanaugite surface and the Mg and Al on the MA-spinel surface chemically reacted with OHA. However, under alkaline conditions, OHA mainly reacted with the Ti and Ca on the perovskite surface, the Ca and Mg on the titanaugite surface, and Mg and Al on the MA-spinel surface.

(4) The results of the artificially mixed mineral flotation experiments show that the concentrate of TiO_2 grade increased from 19.73% to 30.18% at pH 5.4, and a weakly acidic solution is the appropriate condition for the flotation separation of perovskite from titanaugite and MA-spinel.

(5) The results of the modified slag flotation experiments show that the concentrate of TiO_2 grade increased from 18.13% to 23.88% at pH 5.4, and OHA displays selectivity toward perovskite in the modified slag flotation, but the consumption of H_2SO_4 is very high. The $CaSO_4$ precipitate covered on the mineral surfaces results in poor TiO_2 grade and recovery, and effective perovskite flotation processes of modified slag need be further researched.

Acknowledgments: This study was financially supported by the Fund of State Key Laboratory of Mineral Processing (BGRIMM-KJSKL-2015-07), the Opening Project of Key Laboratory of Solid Waste Treatment and Resource Recycle, Ministry of Education (13zxsk06, 14tdgk04), and the Doctoral Foundation Project of Southwest University of Science and Technology (16zx7129). The authors appreciate Tiefeng Peng for his professional language editing.

Author Contributions: Wangwei Wang, Yangge Zhu and Wu Yan conceived and designed the experiments; Shiqiu Zhang and Yang Huang performed the experiments and analyzed the data; Jie Deng contributed reagents and materials; Wangwei Wang and Shiqiu Zhang wrote the paper.

Conflicts of Interest: The authors declare no conflict of interest.

References

1. Zhang, J.-L.; Xing, X.-D.; Cao, M.-M.; Jiao, K.-X.; Wang, C.-L.; Ren, S. Reduction Kinetics of Vanadium Titano-Magnetite Carbon Composite Pellets Adding Catalysts Under High Temperature. *J. Iron Steel Res. Int.* **2013**, *20*, 1–7. [CrossRef]
2. Hou, T.; Zhang, Z.; Ye, X.; Encarnacion, J.; Reichow, M.K. Noble gas isotopic systematics of Fe–Ti–V oxide ore-related mafic–ultramafic layered intrusions in the Panxi area, China: The role of recycled oceanic crust in their petrogenesis. *Geochim. Cosmochim. Acta* **2011**, *75*, 6727–6741. [CrossRef]
3. Pan, F.; Zhu, Q.-S.; Du, Z.; Sun, H.-Y. Oxidation Kinetics, Structural Changes and Element Migration during Oxidation Process of Vanadium-Titanium Magnetite Ore. *J. Iron Steel Res. Int.* **2016**, *23*, 1160–1167. [CrossRef]
4. Han, G.-H.; Jiang, T.; Zhang, Y.-B.; Huang, Y.-F.; Li, G.-H. High-Temperature Oxidation Behavior of Vanadium, Titanium-Bearing Magnetite Pellet. *J. Iron Steel Res. Int.* **2011**, *18*, 14–19. [CrossRef]
5. He, S.; Sun, H.; Tan, D.G.; Peng, T. Recovery of Titanium Compounds from Ti-enriched Product of Alkali Melting Ti-bearing Blast Furnace Slag by Dilute Sulfuric Acid Leaching. *Procedia Environ. Sci.* **2016**, *31*, 977–984. [CrossRef]
6. Zhang, L.; Zhang, L.N.; Wang, M.Y.; Li, G.Q.; Sui, Z.T. Recovery of titanium compounds from molten Ti-bearing blast furnace slag under the dynamic oxidation condition. *Miner. Eng.* **2007**, *20*, 684–693. [CrossRef]
7. Li, J.; Zhang, Z.T.; Wang, X.D. Precipitation behaviour of Ti enriched phase in Ti bearing slag. *Ironmak. Steelmak.* **2012**, *39*, 414–418. [CrossRef]
8. Guo, Z.Z.; Lou, T.P.; Zhang, L.; Zhang, L.N.; Sui, Z.T. Precipitation and growth of perovskite phase in titanium bearing blast furnace slag. *Acta Metall. Sin.* **2007**, *20*, 9–14. [CrossRef]

9. Lou, T.; Yuhai, L.I.; Liaosha, L.I.; Sui, Z. Study of precipitation of perovskite phase from the oxide slag. *Acta Metall. Sin.* **2000**, *36*, 141–144.
10. Li, L.S.; Sui, Z.T. Physical Chemistry Behavior of Enrichment Selectivity of TiO_2 in Perovskite. *Acta Phys. Chim. Sin.* **2001**, *17*, 845–849.
11. Li, Y.; Lou, T.; Sui, Z. The effects of heat-treatment on precipitate behavior of the perovskite phase. *Acta Metall. Sin.* **1999**, *35*, 1130–1134. (In Chinese)
12. Zhang, S.; Wang, W.; Yan, W.; Deng, J.; Huang, Y. Effects of heat treatment conditions on precipitation behavior of perovskite in the Titanium-bearing blast furnace slag. *Iron Steel Vanadium Titan.* **2016**, *37*, 8–14. (In Chinese)
13. Wu, X.Q.; Zhu, J.G. Selective flotation of cassiterite with benzohydroxamic acid. *Miner. Eng.* **2006**, *19*, 1410–1417. [CrossRef]
14. Crumbliss, A.L. Iron bioavailability and the coordination chemistry of hydroxamic acids. *Coord. Chem. Rev.* **1990**, *105*, 155–179. [CrossRef]
15. Chen, G.L.; Tao, D.; Ren, H.; Ji, F.F.; Qiao, J.K. An investigation of niobite flotation with octyl diphosphonic acid as collector. *Int. J. Miner. Process.* **2005**, *76*, 111–122. [CrossRef]
16. Agrawal, Y.K. Hydroxamic Acids and Their Metal Complexes. *Russ. Chem. Rev.* **1979**, *48*, 948–963. [CrossRef]
17. Ni, X.; Liu, Q. The adsorption and configuration of octyl hydroxamic acid on pyrochlore and calcite. *Colloids Surf. A Physicochem. Eng. Asp.* **2012**, *411*, 80–86. [CrossRef]
18. Meng, Q.; Feng, Q.; Shi, Q.; Ou, L. Studies on interaction mechanism of fine wolframite with octyl hydroxamic acid. *Miner. Eng.* **2015**, *79*, 133–138. [CrossRef]
19. Zhou, F.; Yan, C.; Wang, H.; Sun, Q.; Wang, Q.; Alshameri, A. Flotation behavior of four C18 hydroxamic acids as collectors of rhodochrosite. *Miner. Eng.* **2015**, *78*, 15–20. [CrossRef]
20. Pavez, O.; Brandao, P.R.G.; Peres, A.E.C. Adsorption of oleate and octyl-hydroxamate on to rare-earths minerals. *Miner. Eng.* **1996**, *9*, 357–366. [CrossRef]
21. Sreenivas, T.; Manohar, C. Adsorption of Octyl Hydroxamic Acid/Salt on Cassiterite. *Miner. Process. Extr. Metall. Rev.* **2000**, *20*, 503–519. [CrossRef]
22. Wu, M.-Z.; Lü, H.-H.; Liu, M.-C.; Zhang, Z.-L.; Wu, X.-R.; Liu, W.-M.; Wang, P.; Li, L.-S. Direct extraction of perovskite $CaTiO_3$ via efficient dissociation of silicates from synthetic Ti-bearing blast furnace slag. *Hydrometallurgy* **2017**, *167*, 8–15. [CrossRef]
23. Han, C.; Liu, J.; Yang, W.; Wu, Q.; Yang, H.; Xue, X. Enhancement of photocatalytic activity of $CaTiO_3$ through HNO_3 acidification. *J. Photochem. Photobiol. Chem.* **2016**, *322–323*, 1–9. [CrossRef]
24. Sreenivas, T.; Padmanabhan, N.P.H. Surface chemistry and flotation of cassiterite with alkyl hydroxamates. *Colloids Surf. A Physicochem. Eng. Asp.* **2002**, *205*, 47–59. [CrossRef]
25. Ma, J.W.; Sui, Z.T.; Chen, B.C.; Nie, Y.F. Flotation behavior and mechanism on perovskite in Ti-bearing blast furnace slag. *Chin. J. Nonferrous Met.* **2002**, *12*, 171–177. (In Chinese)
26. Fan, X.; Waters, K.E.; Rowson, N.A.; Parker, D.J. Modification of ilmenite surface chemistry for enhancing surfactants adsorption and bubble attachment. *J. Colloid Interface Sci.* **2009**, *329*, 167–172. [CrossRef] [PubMed]
27. Mehdilo, A.; Irannajad, M.; Rezai, B. Effect of crystal chemistry and surface properties on ilmenite flotation behavior. *Int. J. Miner. Process.* **2015**, *137*, 71–81. [CrossRef]
28. Bahri, Z.; Rezai, B.; Kowsari, E. Evaluation of cupferron on the selective separation of gallium from aluminum by flotation: The separation mechanism. *Miner. Eng.* **2016**, *98*, 194–203. [CrossRef]
29. Ikumapayi, F.; Makitalo, M.; Johansson, B.; Rao, K.H. Recycling of process water in sulphide flotation: Effect of calcium and sulphate ions on flotation of galena. *Miner. Eng.* **2012**, *39*, 77–88. [CrossRef]
30. Al-Fariss, T.F.; Arafat, Y.; Abd El-Aleem, F.A.; El-Midany, A.A. Investigating sodium sulphate as a phosphate depressant in acidic media. *Sep. Purif. Technol.* **2014**, *124*, 163–169. [CrossRef]